Terminal Shapes of Ablating Bodies

DAVID T. WILLIAMS*
University of Florida, Gainesville, Fla.

A STUDY of the fluid dynamics of ablating bodies has been pursued at the University of Florida for the past three years. In this study, blocks of soluble material have been mounted on suitable supports located under water on the prow of a small skiff, which is then propelled at known constant speed by use of an outboard motor. The changes in shapes of the soluble specimens have been observed as a function of the boat speed, the time, the initial model shape, and its material composition.[1]

In early experiments, models of salt which had an initial cylindrical symmetry about the direction of relative motion of the water—square-ended cylinders, or ogives—were found to erode to a shape that seemed to change very little with time but for scale. The shape could be described in terms of the coordinates x and y, where the lateral dimension y is measured vertically from the line of cylindrical symmetry of the model at a distance x measured along that axis from the forward tip of the shape. The relation between y and x was found to be

$$y = ax^n \tag{1}$$

where a and n are constant. Figure 1 shows one such shape, referred to hereafter as a "terminal shape," defined as a shape that is constant with time but for scale.

Repetition of the same type of experiment on blocks of salt having a two-dimensional conformation (wing shapes projecting vertically from a plane parallel to the flow direction) were found to erode likewise to a terminal shape, the section normal to the wing axis being described by an equation of the form of Eq. (1).

The salt from which the models were machined is a microcrystalline, fairly compact salt (about 6% of voids), formed by hydraulic compression of pure kiln-dried sodium chloride crystals with less than 2% admixture of certain dietary minerals and sold in 50-lb cakes for cattle feeding. Other models also were made of heavy sugar-syrup cast in molds and cooled to form noncrystalline sugar-glass shapes of the same general type as the salt models. All sugar-glass specimens were found, after ablation, to be covered with pimples roughly $\frac{1}{4}$ in. in diameter and $\frac{1}{8}$ in. high. The gross shapes of the sugar-glass models were found to reduce to terminal shapes of the form of Eq. (1).

When all the data obtained by use of salt and sugar-glass models, both axially symmetric and with two-dimensional symmetry, were collated and compared, it was found that the exponent n of Eq. (1) was roughly the same for all the different conditions—type of symmetry, material, as well as water speed and time. The value of n, more specifically, could be duplicated in successive plots of the data from the same shape to about 6%, and the various sets of data showed the same value of n to about the same precision. Figure 2 shows the log-log plot of two typical samples of the data; Table 1 summarizes all the observations.

The value $n = 0.8$ was computed as the mean value of n taken from all the data. It is not altogether certain that the deviations of the various individual slopes of the data points on log-log plots are random in nature. It is believed at least that the values of n in Eq. (1) are the same within less than 6% as the mean value; the average deviation turns out to be less than 3%. The slopes were always taken from the portion

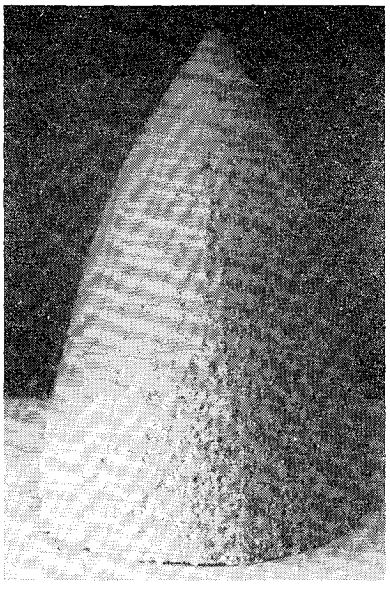

Fig. 1 Photograph of typical terminal shape, cylindrically symmetrical alt model

of the shapes nearest the forward tip, for reasons that are now to be discussed.

It is clear that any shape described by an equation of the form of Eq. (1) for a fixed value of the exponent n is a terminal shape as the term is defined here: for a scale factor, R, in principle always can be found such that the constant a can be reduced to any arbitrary value. Thus, consider two shapes described by $y_1 = a_1x_1^n$ and $y_2 = a_2x_2^n$. A scale factor R always can be found such that

$$y_2/R = (a_2/R^{1-n})(x_2/R)^n = a_1(x_2/R)^n$$

A number of statements can be made relating to terminal shapes of ablating bodies as observed:

1) Terminal shapes are expected to be observed mainly near the front end of ablating bodies. Ablation rates tend to decrease with increasing distance back from the stagnation point. Hence the departure from the initial shape will be less at distances further from the tip, and if any departure from the terminal shape is to be anticipated, it would be greater further from the tip.

2) Leading faces of ablating bodies tend to reduce to a reasonably sharp point or edge on soluble models and a blunt, generally spherical (or circular) shape on thermally ablated models.

3) The scale R of sugar-glass specimens was found to decrease with time, whereas it was more nearly constant with time on salt specimens.

4) Terminal shapes of the type observed here were found only under conditions where no fixed separation point of the flow from the surface could be expected to exist. Where a stationary region of separation was predictable, a pit or depression generally was found to develop at that point, and terminal shapes of the type discussed were never formed under such circumstances. In short, the ablation rate was higher under a stationary vortex on a flat surface than on a flat surface where no stationary vortex was to be found. Therefore, terminal shapes as discussed are characteristic only of ablation forward of any possible stationary region of flow separation.

It seems natural to inquire whether stationary shapes might exist over surfaces subject to thermal ablation as in re-entry vehicles. One answer is quite clearly valid: some shapes subject to ablation in a rocket blast certainly do not change rapidly in conformation with time; therefore, one would expect a shape that is a terminal one, in the formal sense of the term, to be formed on samples subject to ablation in a rocket blast, for more or less extended periods.

Beyond this quick answer, it may be remarked that there are natural objects that are reputed to have been subject to

Received by ARS November 7, 1962. This work was supported by the National Science Foundation.

* Professor, Department of Aerospace Engineering, College of Engineering. Member AIAA.

Table 1 Results of solution-ablation terminal shape experiments

Material	Initial nose shape	Water speed, knots	Time, min	Slope n of log-log curve
Axially symmetric shapes				
Salt	ogive	4.8	21	0.763
Salt	flat	4.8	21	0.826
Salt	ogive	4.8	15	0.767
Salt	ogive	4.8	21	0.758
Sugar-glass	cone-cylinder	7.13	30	0.831
Sugar-glass	cone-cylinder	7.13	20	0.857
			Mean	0.797 ± 0.016
Wing shapes				
Salt	semicylinder	4.75	3	0.788
Salt	ogive	3.9	4	0.826
Salt	ogive	5.13	3	0.800
Salt	flat, with bevel corner	5.13	4.6	0.813
Sugar-glass	ogive	5.3	12	0.763
Sugar glass	flat	5.3	15	0.781
Sugar-glass	semicylinder	5.3	10	0.846
Sugar glass	semicylinder	5.3	15	0.833
			Mean	0.806 ± 0.007

re-entry under such conditions that they may be expected to have terminal shapes. These objects are tektites and, in particular, australites, which are believed by some to have been ejected from the moon and have entered the earth's atmosphere at speeds somewhat in excess of earth escape velocity.[2]

In order to see whether australites have shapes of the form of Eq. (1), three Charlotte Waters, Australia, tektites were borrowed from E. P. Henderson of the National Museum of the Smithsonian Institution, Washington, D. C., and were measured by use of a micrometer microscope to determine the shape. The logarithmic plot of lateral dimension as a function of the longitudinal dimension is shown in Fig. 3. In the same plot are presented data taken from Refs. 3 and 4 for a teflon rod and a Kel-F cone exposed to supersonic thermal ablating flow. It is clear that the tektite data are very well described by straight lines on the log-log plot; the slopes are 2.34, 2.00, and 1.91 for the three samples. The samples of plastic materials subject to ablation in supersonic flow presumed to be at Mach numbers much below those for re-entry are describable by straight lines near the forward tip. The half of the log plots further from the tip which constitute the bulk of the shapes and the most reliable data are also well described by straight lines on the log-log plot. The slopes near the tip are 1.85 for both plastic models; further from the tip the slopes are 1.94 and 2.27 for the teflon and Kel-F samples, respectively. The two plastic shapes show the same value of slope as in the tektite data, to 15% if the larger slopes are used. It should be noted that neither plastic shape was measured far enough back of the tip to show any noticeable influence of the original shape before ablation.

These data are considered to indicate that bodies subject to ablation such as would exist during re-entry from orbit do indeed tend to take on a terminal shape describable by an equation of the form of Eq. (1). The value of the exponent is considered to lie within 15% or so of the value 2.1, and, within this range of uncertainty, the shapes of subliming models subject to ablating flow of much smaller Mach numbers have the same exponent n, within the rather broad limits of uncertainty in the measurement of the slopes. The deviation between n for rocket-ablated plastic shapes and for the tektites measured here is, in short, considered to lie barely within the range of uncertainty of slope measurement. The value of n observed here for thermally ablated specimens is more than twice as great as the value for n of 0.8 valid for the terminal shapes formed on soluble models by water flow.

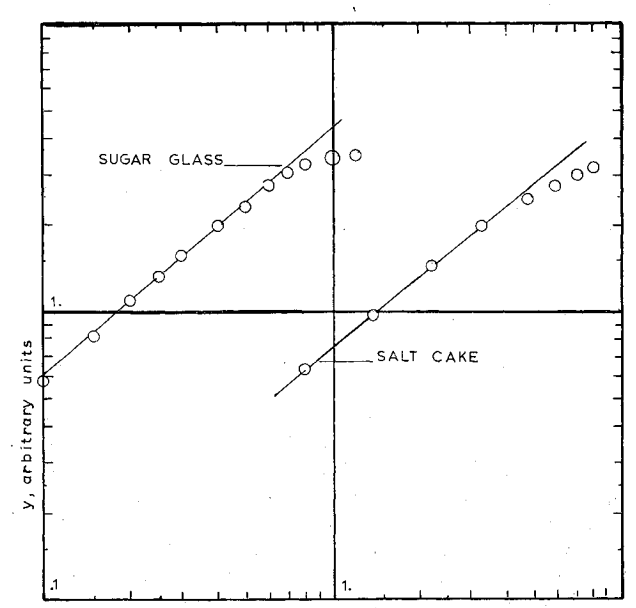

Fig. 2 Sample data, cylindrically symmetrical terminal shapes

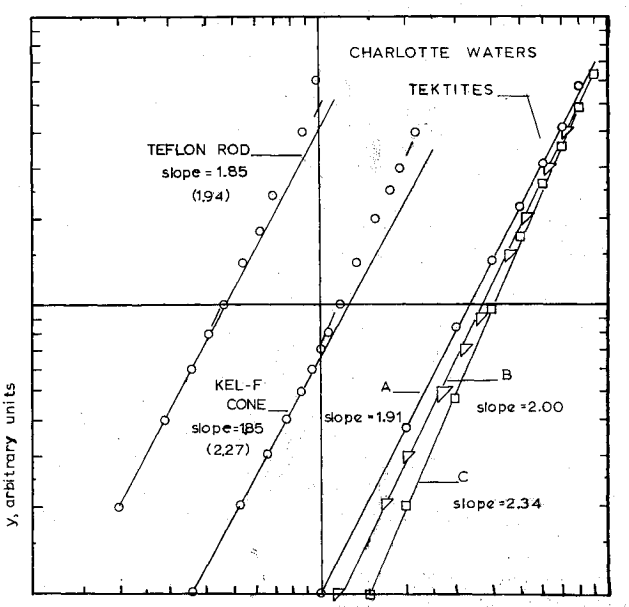

Fig. 3 Terminal shapes of ablating bodies: A, 4.21 *g*; B, 4.43 *g*, *a*; C, 4.43 *g*, *b*

References

[1] Williams, D. T., "A fluid-dynamic mechanism of meteorite pitting," Smithsonian Contrib. Astrophys. **3**, 47–67 (1959).

[2] Chapman, D. R., "Recent re-entry research and the cosmic origin of tektites," Nature **188**, 353 (1960).

[3] Georgiev, S., Hidalgo, H., and Adams, M. C., "On ablation for the recovery of satellites," *1959 Heat Transfer and Fluid Dynamics Institute* (Stanford University Press, Stanford, Calif., 1959), pp. 171–180.

[4] Gregorek, G. M., "The ablation of axisymmetric models in a hypersonic air stream with stagnation temperature to 2300° R," Army Ballistic Missile Agency Contract No. DA33-019-ORD-2314, Final Rept. TN(ALOSU)460-4, Part I (May 1960).

Criterion for Vibrational Freezing in a Nozzle Expansion

R. PHINNEY*

Martin Company, Baltimore, Md.

THE flow of a dissociating gas has been studied in some detail, and criteria for the point at which the recombination process freezes have been developed and verified.[1–3] The purpose of this note is to show that the same criterion can be used to predict vibrational freezing as well. This vibrational criterion is checked against numerical data given in Ref. 4.

The criterion of Bray is nearly the same as that of Refs. 1 and 3. For convenience, the later formulation is used as the basis of the present work. The rate equation governing the dissociational relaxation process can be written as

$$d\alpha/dx = -(\alpha - \alpha_e)/r \tag{1}$$

The notation is that of Refs. 2 and 3, where r is a relaxation distance depending on temperature, density, and degree of dissociation α. The subscript e indicates the local equilibrium value. An argument is given to show that the reaction will freeze at the point in the flow where

$$d\alpha_{e\infty}/dx = \alpha_{e\infty}/r_{e\infty} \tag{2}$$

The subscript $e\infty$ indicates the local value for the equilibrium (infinite rate) nozzle flow. In other words, the criterion requires only the equilibrium solution to establish the freezing point.

Define D to be the dissociation energy per mole so that $\alpha D = E_{\text{diss}}$ is the dissociation energy present in the flow. If both sides of Eqs. (1) and (2) are multiplied by D, then they take the form

$$dE_{\text{diss}}/dx = -(E_{\text{diss}} - E_{\text{diss}\,e})/r \tag{3}$$

$$dE_{\text{diss}\,e\infty}/dx = E_{\text{diss}\,e\infty}/r_{e\infty} \tag{4}$$

But Eq. (3) is in the same form that the vibrational relaxation equation usually takes [Eq. (5) of Ref. 4]:

$$dE_{\text{vib}}/dx = -(E_{\text{vib}} - E_{\text{vib}\,e})/r \tag{5}$$

so that it is natural to try the modified form of Eq. (4) to predict the vibrational freezing point:

$$dE_{\text{vib}\,e\infty}/dx = E_{\text{vib}\,e\infty}/r_{e\infty} \tag{6}$$

Reference 4 gives the numerical results for a nozzle flow of a step by step integration of Eq. (5) together with the other fluid

Received by ARS November 6, 1962.

* Research Scientist, Space Systems Division.

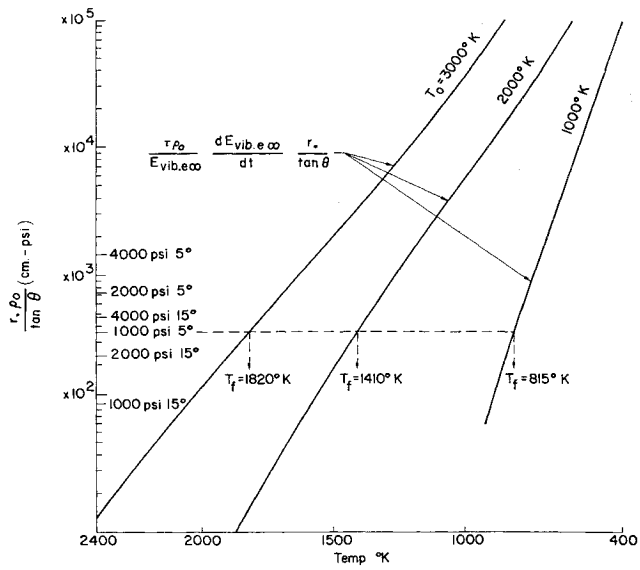

Fig. 1 Curves for the determination of freeze temperature

dynamical equations to obtain the asymptotic (freeze point) value of the vibrational temperature T_f. For comparison, the freeze point has been determined graphically using Eq. (6), which is used in the form

$$\frac{\tau p_0}{E_{\text{vib}\,e\infty}} \frac{dE_{\text{vib}\,e\infty}}{dt} \frac{r_*}{\tan\theta} = \frac{p_0 r_*}{\tan\theta} \tag{7}$$

where r_* is the throat radius in centimeters, θ is the half angle of the conical nozzle, p_0 is the stagnation pressure in atmospheres, and τ is the vibrational relaxation time. The flow with vibrational equilibrium can be calculated in nondimensional form so that for a given stagnation temperature the stagnation pressure enters only in the parameter $p_0 r_*/\tan\theta$, and the left-hand side of Eq. (7) is a function of temperature only. In plotting the curve, the same gas data and dependence of τ on temperature were used as were used in Ref. 4. The result is shown in Fig. 1. Table 1 gives the comparison between the freeze point temperature as given in Ref. 4 and as determined from Fig. 1. As can be seen, the agreement is quite good considering the fact that both Ref. 4 and the present work have used approximate procedures and fairing to achieve the final result.

Table 1 Comparison of exact and approximate values of vibrational freezing temperature

T_0, °K	θ	p_0, psi	T_f (Ref. 4), °K	T_f (present method), °K
3000	5	1000	1908	1820
	5	2000	1752	1690
	5	4000	1612	1560
	15	1000	2140	2205
	15	2000	1995	1900
	15	4000	1853	1775
2000	5	1000	1515	1410
	5	2000	1380	1310
	5	4000	1272	1210
	15	1000	1712	1565
	15	2000	1577	1465
	15	4000	1450	1370
1000	5	1000	912	815
	5	2000	850	760
	5	4000	770	710
	15	1000	955	890
	15	2000	922	845
	15	4000	872	795